Improving Indoor Positioning Accuracy Using RIS-based RSS Optimization

Somayeh Bazin, Keivan Navaie
School of Computing and Communication, Lancaster University, UK
{s.bazin, k.navaie}@lancaster.ac.uk

***Abstract*—In the Received Signal Strength (RSS) based Indoor Positioning Systems (IPS), the position of a receiver is estimated by comparing its RSS values with a fingerprint. The fingerprint is a dataset including the measured RSS values at pre-planned Reference Points (RP) for a set of reference transmitters. For a given RPs' spatial distribution, the RSS values are however affected by the intrinsic temporal and spatial uncertainties in the indoor wireless channel, hence constraining the positioning accuracy. To address this issue, we propose an algorithm to pre-design the RSS values at each RP using Reconfigurable Intelligent Surface (RIS) technology. In the proposed method, the RIS reflection coefficients are obtained to maximize the difference between the RSS values between the RPs. The simulation results confirm that even with a relatively small number of RIS elements, the proposed method significantly improves the IPS efficiency.**

***Index Terms*—Indoor positioning systems, Re-configurable intelligent surface, Received signal strength.**

I. Introduction

Location-based services are essential in new services that significantly improve the quality of life. Examples include a wide range of applications from safety and security to marketing and e-health. Nevertheless, in indoor environments, the performance of Global Navigation Satellite Systems (GNSS) is often unsatisfactory.

One of the main techniques for Indoor Positioning Systems (IPS) is the Received Signal Strength (RSS)-based positioning. This method is not only efficient but also easily implementable using existing WiFi infrastructures [1]. However, due to the high level of spatial correlation in the RSS values [2], it is challenging to differentiate between closely located Reference Points (RP) as they might receive nearly similar RSS values.

The positioning accuracy is also affected by the dynamic nature of indoor environments and stochastic wireless signal propagation resulting in stochastic RSS values. Therefore, the accuracy of an RSS-based positioning system is contingent upon the distribution of RSS values at the RPs. To address this issue, in this paper we argue that there exists a favorable distribution that maximizes the difference between the RSS values across all RPs. Hereafter we referred to this distribution as the Maximum Differentiated RSS (MDRSS).

Previous research also attempted to manipulate the RSS distribution by using different WLAN interfaces [3] or proposing improved RSS combinations [4]. Using Re-configurable Intelligent Surface (RIS) also enables customizing the RSS distribution by directly adjusting the signal propagation [5]. RIS is a planar surface consisting of passive reflecting elements that can be configured to achieve specific objectives.

Several previous studies have explored the use of RIS for indoor positioning [6]–[8]. For instance, [6] utilized the diversity provided by RIS to enhance the accuracy of radio maps, resulting in a 33% improvement. Similarly, in [7], the potential for accuracy enhancement by combining ultra-wideband (UWB) and RIS in a single access point (AP) was demonstrated. Also, [8], investigated the achievable accuracy improvement by customizing the RSS distribution using RIS. In a multi-user scenario, RIS configuration was also optimized in [8] based on the user's RSS values. In their approach time division multiplexing (TDM) is necessary to exclusively allocate a time slot and RIS configuration to each user.

Despite the potential benefits of using RIS for indoor positioning, obtaining an optimal (or near-optimal) RIS configuration to achieve maximum accuracy is challenging. Achieving maximum accuracy in RIS-assisted indoor positioning involves minimizing the number of false positioning incidents. Such an incident occurs when the Euclidean distance between the measured RSS and the fingerprint of a reference point (RP) is less than that of the distance between the measured RSS and its own RP's fingerprint. This can be due to environmental noise or similar RSS values in neighboring RPs. To address this issue, the RIS should be configured to achieve MDRSS in the environment.

In this paper, we propose a novel Static Reconfiguration Algorithm (SRA) to determine the corresponding RIS settings. The optimization problem that maximizes the minimum distances in the coverage area is used to obtain the RSS distribution that results in MDRSS. Simulation results demonstrate that the proposed SRA significantly increases the positioning accuracy by almost 40%, with a standard deviation of RSS of 8. Following is the list of our contributions:

- Our proposed method is inspired by [8] where the maximum differentiated RSS distribution is utilized to enhance accuracy. Nevertheless, our proposed method (SRA) further supports an unlimited number of users without requiring any reconfiguration of the RIS.
- The required number of RIS elements in SRA is relatively low. Hence, the computation complexity of SRA is lower than the state-of-the-art.
- In contrast to the previous works (e.g., [6]–[8]), the multipath impact is incorporated in the design of SRA.

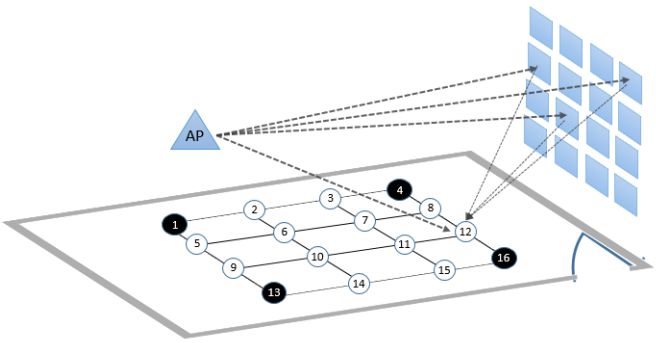

Fig. 1. Schematic of signal propagation model with RIS.

- Compared to the state-of-the-art, SRA significantly increases the localization accuracy, even in a rich scattering indoor environment.

The rest of this paper is organized as the following. In Section II, the system model is presented. Problem formulation is presented in Section III where we present the problem of obtaining RIS coefficients to achieve MDRSS for the coverage area. Section IV presents SRA to obtain the relative coefficients of RIS elements. The simulation results comparing SRA with the state-of-the-art are also presented in Section V followed by the conclusions drawn in Section VI.

II. SYSTEM MODEL

A. RIS Assisted Signal Propagation Model

Fig. 1 represents a schematic of an indoor environment, where the RIS panels are used to improve localization accuracy. Different RPs are indicated by different numbers, where they receive signals from RIS and AP.

The indoor environment often has a rich multipath signal propagation. The channel impulse response is

$$h(t) = \sum_{k} \alpha_k e^{j\theta_k} \delta(t - \tau_k), \tag{1}$$

where α_k, θ_k, τ_k are gain, a uniformly distributed random variables phase shift [9], and propagation delay of each individual path, respectively. Furthermore, k is the path's index out of total K paths and δ is the Dirac delta function. The rate of environmental change is assumed to be far lower than the rate of signaling. Thus, α_k, θ_k and τ_k are considered time-invariant random variables. Suppose that the environment includes I RPs, the received signal at ith RP is

$$y_{\mathrm{AP-RP_i}}(t) = \sum_{k} \alpha_{k,i} g(t - \tau_{k,i}) e^{j\left(\omega(t-\tau_{k,i})+\theta_{k,i}\right)}, \tag{2}$$

where ω is an angular frequency and $g(t)$ is a baseband pulse which is a periodic square pulse with the width of W and period of T, $T > W$. Also, the values of $\alpha_{k,i}$ and $\tau_{k,i}$ correspond to $\frac{\lambda}{4\pi}.\frac{\sqrt{G_t G_r}}{d}$ and d/C, where λ is the wavelength, d is the distance of transmitter and receiver while the receiver supposed to be at the ith RP, C is the light's speed, and G_t, G_r are power gains of transmitter and receiver respectively.

In the RIS systems, in addition to the aforementioned multipath links, the composite AP-RIS-RP links should also be modeled. RIS consists of N reflector elements, where each receives the propagated signal from an AP and then reflects it according to the following

$$y_{\mathrm{out,n}}(t) = \beta_n y_{\mathrm{in,n}}(t - t_n), \tag{3}$$

where β_n and t_n are adjustable amplitude and delay coefficients of the nth RIS element. Suppose $(\tau_n, \tau'_{n,i})$, $(\alpha_n, \alpha'_{n,i})$, and $(\phi_n, \phi'_{n,i})$ are delay, amplitude, and phase shift of AP-RIS, RIS-RP links', respectively. The signal received at the RP from RIS is

$$y_{\mathrm{AP-RIS}_n-\mathrm{RP}_i}(t) = \sum_{n} \beta_n \alpha_n \alpha'_{n,i} g(t - t_n - \tau_n - \tau'_{n,i}) e^{j\left(\omega(t-t_n-\tau_n-\tau'_{n,i})+\phi_n+\phi'_{n,i}\right)}, \tag{4}$$

or equivalently,

$$y_{\mathrm{AP-RIS}_n-\mathrm{RP}_i}(t) = \sum_{n} B_{n,i} g(t-\mu_{n,i}) e^{j\left(\omega(t-\mu_{n,i})+\theta_{n,i}\right)}, \tag{5}$$

where

$$B_{n,i} = \beta_n \alpha_n \alpha'_{n,i}, \mu_{n,i} = t_n + \tau_n + \tau'_{n,i}, \theta_{n,i} = \phi_n + \phi'_{n,i}. \tag{6}$$

The received signal at each RP consists of Line-of-Sight (LoS) and None-Line-of-Sight (NLoS) components of AP-RP multipath channels and N reflected signal from AP-IRS-RP channels. Thus the final received signal is

$$y_i(t) = \sum_{l=1}^{N+K} B_{l,i} g(t - \mu_{l,i}) e^{j\left(\omega(t-\mu_{l,i})+\theta_{l,i}\right)}. \tag{7}$$

B. RSS Model

Equation (7) shows that RIS adds delayed and amplified versions of the originally transmitted signal to RP. Therefore, at the ith RP,

$$|y_i(t)|^2 = \sum_{l} \sum_{v} B_{l,i} B_{v,i} g(t - \mu_{l,i}) g(t - \mu_{v,i}) e^{j\left(\theta_{l,i}-\theta_{v,i}+\omega(\mu_{l,i}-\mu_{v,i})\right)}, \tag{8}$$

where $\theta_{l,i}$ is a uniformly disturbed random variable. Therefore, (8) is reduced to

$$E_i(t) = \mathrm{E}_\theta \left\{ |y_i(t)|^2 \right\} = \sum_{l}^{K+N} B_{l,i}^2 g^2(t - \mu_{l,i}), \tag{9}$$

where $\mathrm{E}_\theta \{.\}$ denotes expected value with respect to θ and,

$$E_i = \int_{T_1}^{T_2} E_i(t) dt, \tag{10}$$

$T1, T2$, $(T_2 - T_1) < T$, are the starting and ending times of energy measurement. Therefore, RSS at the ith RP is

$$\mathrm{RSS}_i = 20\log_{10} \left(\sum_{l=1}^{K+N} B_{l,i}^2 \int_{T_1}^{T_2} g^2(t - \mu_{l,i}) dt \right) + \xi, \tag{11}$$

where ξ has a normal distribution, i.e., $\mathcal{N}(0, \sigma^2)$ which represents RSS measurement noise [8].

III. Problem Formulation

It is reasonable to assume that the distance between RIS elements is much less than that of RPs. Thus, the RIS can be treated as a single-point receiver and transmitter, hence, $\alpha'_{1,i} = \alpha'_{2,i} = ... = \alpha'_{N,i} = \alpha'_i$, and $\alpha_1 = \alpha_2 = ... = \alpha_N = \alpha$. Substituting (6) in (11) yields

$$\sum_{n=1}^{n=N} \beta_n^2 \int_{T_1}^{T_2} g^2(t-\mu_{n,i})dt = \left(\frac{1}{\alpha^2 \alpha'^2_i}\right)\left\{10^{\text{RSS}_i/20} - \sum_{k=1}^{k=K} B_{k,i}^2 \int_{T_1}^{T_2} g^2(t-\mu_{k,i})dt\right\}, \tag{12}$$

or equivalently,

$$\sum_{n=1}^{n=N} \beta_n^2 \int_{T_1}^{T_2} g^2(t-\mu_{n,i})dt = C_i, \tag{13}$$

where C_is are the values that we aim to adjust to obtain MDRSS. Note that the term, $\mu_{n,i}$, consists of two time delays including t_n which is adjusted by the nth element of RIS, and $\tau_{n,i} = \tau_n + \tau'_{n,i}$.

Generally, the sampling frequency of the wireless signal, f_s, is such that $1/f_s < Dt$, where $Dt = \tau_{u,i} - \tau_{v,i}$ and u and v are any two arbitrary RIS elements. Therefore, signals received at the same RP from different RIS elements, experience different delays due to different t_n values. Also, signals received at different RPs from the same RIS element experience different delays due to the different $\tau_{n,i}$. Let $\int_{T_1}^{T_2} g^2(t-\mu_{n,i})dt \triangleq G(\tau_{n,i}, t_n)$, we write,

$$\begin{cases} \beta_1^2 G(\tau_{1,1}, t_1) + \beta_2^2 G(\tau_{2,1}, t_2) + ... + \beta_N^2 G(\tau_{N,1}, t_N) & = C_1 \\ \beta_1^2 G(\tau_{1,2}, t_1) + \beta_2^2 G(\tau_{2,2}, t_2) + ... + \beta_N^2 G(\tau_{N,2}, t_N) & = C_2 \\ & \cdot \\ & \cdot \\ & \cdot \\ \beta_1^2 G(\tau_{1,I}, t_1) + \beta_2^2 G(\tau_{2,I}, t_2) + ... + \beta_N^2 G(\tau_{N,I}, t_N) & = C_I \end{cases}$$

which can be represented as the following matrix equation,

$$\mathbf{G\Upsilon} = \mathbf{C}, \tag{14}$$

hence,

$$\mathbf{\Upsilon} = \mathbf{G^{-1}C}, \tag{15}$$

where $\mathbf{G}$ is an $I \times N$ matrix and $\mathbf{\Upsilon} = [\beta_1^2, \beta_2^2, \beta_3^2, ..., \beta_N^2]^T$.

The RIS coefficients, β_n, and t_n need to be determined such that the obtained C_is result in MDRSS. Conventionally, finding the RIS delays and amplitudes that result in the most distinct RSS values in the radio map, requires a brute-force search among all possible combinations of the coefficients.

To address this issue we propose SRA with significantly lower computational complexity. SRA composes of two steps. In the first step, the delay of each element is adjusted so that for each RP, instead of all RIS elements, an exclusive subset of elements is involved for determining the customized RSS.

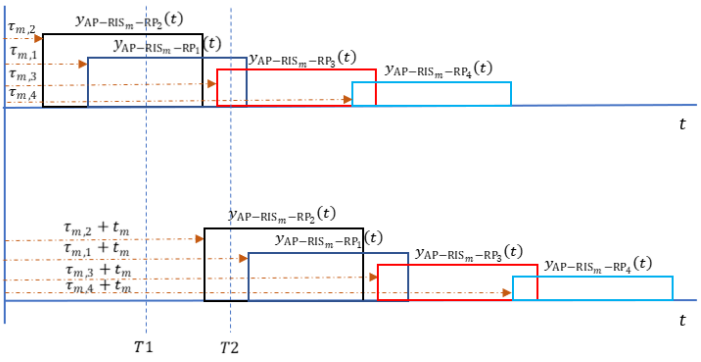

Fig. 2. RIS delay determination.

This approach considerably reduces the complexity. Moreover, allocation of an exclusive subset of RIS elements to each RP ensures none-singularity of $\mathbf{G}$. In the second step, we then determine the constraints that ensure the positive solution for (14). Finally, by applying these constraints the solution to the optimization problem that results in MDRSS is obtained.

IV. Static Reconfiguration Algorithm

A. RIS Delay

For static reconfiguration of RIS, different sets of relative RIS coefficients are assigned to different RPs without requiring the RIS to be reconfigured. This means that a unique set of coefficients is obtained for each RP. Hence, for any arbitrary pair of RPs denoted as (i, j), there exist $\boldsymbol{\nu}_i, \boldsymbol{\nu}_j$, such that

$$\boldsymbol{\nu}_i \subseteq \mathbf{\Upsilon}, \boldsymbol{\nu}_j \subseteq \mathbf{\Upsilon}, \boldsymbol{\nu}_i \neq \boldsymbol{\nu}_j.$$

Let $\boldsymbol{\mu}_m$ be a vector of delays including $\tau_{m,i}$ and t_m:

$$\boldsymbol{\mu}_m \triangleq [t_m + \tau_{m,1}, t_m + \tau_{m,2}, t_m + \tau_{m,3}, ..., t_m + \tau_{m,I}]^t,$$

and $\tau_{m,k} = \min_i\{\tau_{m,i}\}$. We then define $\mathbf{G}_{(i,m)}$,

$$\mathbf{G}_{(i,m)} \triangleq \int_{T1}^{T2} g^2(t - \boldsymbol{\mu}_{m(i)}),$$

To determine the exclusive subset of RIS elements for each RP, t_m is then adjusted so that $t_m + \tau_{m,k} = T_2 - \epsilon$, hence:

$$\mathbf{G}_{(i,m)} = \begin{cases} \int_{T2-\epsilon}^{T2} g^2(t - \boldsymbol{\mu}_{m(k)})dt & \text{if } i = k, \\ 0 & \text{if } i \neq k. \end{cases}, \tag{16}$$

where ϵ is set such that:

$$\tau_{m,i} + t_m = \begin{cases} < T2 & \text{if } i = k, \\ \geq T2 & \text{if } i \neq k. \end{cases}. \tag{17}$$

Subject to the constraints defined in (17) and (16), the mth element of the RIS (RIS_m) is adjusted to impose the MDRSS for the kth RP (RP_k). Fig. 2 illustrates the delay determination of RIS_m in the SRA. As it is seen, after adjusting t_m, the signal received from RIS_m is only involved in the determination of the RSS of RP_2. As a result, the amplitude coefficient of

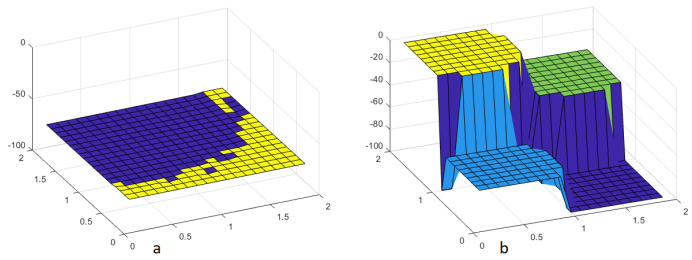

Fig. 3. (a): Radio map without RIS, (b): Radio map with RIS

RIS_m can be changed to adjust the RSS at RP_2. In the SRA, RIS_m is considered as the associated element for RP_k (e.g., $k = 2$ in Fig. 2). The associated element is the element whose amplitude directly adjusts the MDRSS at that specific RP. By extending this process to all N different vectors of $\boldsymbol{\mu}$, a one-to-one correspondence between all RPs and their associated RIS elements is established. This one-to-one correspondence serves two purposes: (i) it ensures that the sets of RIS elements involved in the determination of the RSS of each RP are mutually exclusive, and (ii) it enables the customization of the MDRSS with the minimum number of RIS elements required.

Nevertheless, there might exist other RIS elements in $\boldsymbol{\nu}_k$ for which by adjusting t_m the vector $\boldsymbol{\nu}_k$ is also updated so that $\beta_m^2 \in \boldsymbol{\nu}_k$. This is a result of the one-to-one correspondence implemented by the SRA. The delay coefficients for the RIS elements are generated such that once an element is associated with an RP, the other elements cannot be associated with the same RP again. This is achieved through the calculation of the required delay for each RIS element, which is explained in the following.

Suppose $\tau_{m,k}$ is the minimum delay of μ_m which corresponds the RIS_m to be associated to the RP_k, and $\tau'_{m+1,k}$ is the minimum delay of μ_{m+1}. Here instead of setting $t_{m+1} + \tau'_{m+1,k} = T2 - \epsilon$ which leads to $\text{RIS}_{(m+1)}$ associates to RP_k again, we set $t_{m+1} + \tau'_{m+1,k'} = T2 - \epsilon$, where $\tau'_{m+1,k'}$ is the second minimum delay. Therefore:

$$\mathbf{G}_{(i,m+1)} = \begin{cases} \int_{T2-\epsilon'}^{T2} g^2(t - \boldsymbol{\mu}_{m+1(k)})dt & \text{if } i = k, \\ \int_{T2-\epsilon}^{T2} g^2(t - \boldsymbol{\mu}_{m+1(k')})dt & \text{if } i = k', \\ 0 & \text{if } i \neq (k, k'). \end{cases}, \tag{18}$$

where $\epsilon' = \epsilon + (\tau'_{m+1,k'} - \tau'_{m+1,k})$. Similarly, for the mth column of $\mathbf{G}_{(:,m)}$, the nonzero elements are obtained for $i = k$ and, $\forall j$ that $\tau_{m,j} <= \tau_{m,k}$, provided that $k \notin \boldsymbol{\Theta}$, where $\boldsymbol{\Theta}$ is a set of nonzero indexes from $\mathbf{G}_{(:,1)}$ to $\mathbf{G}_{(:,m-1)}$. Furthermore, it can be inferred from (18) that $\mathbf{G}_{(k,m+1)} \geq \mathbf{G}_{(k',m+1)}$, which is later used to define the constraints ensuring $\boldsymbol{\Upsilon} > 0$.

B. Maximizing RSS Differentiation with C_i Determination

This section aims to determine C_i that yields MDRSS such that $\boldsymbol{\Upsilon} > 0$. Suppose the $[\text{RSS}_1, \text{RSS}_2, ..., \text{RSS}_I]^t$ is a vector of all RSS values of an environment. The following optimization problem is required to achieve MDRSS.

$$\max_{C_i} \min \left\{ \left| \sum_{i=1}^{I} \mathbf{f}_{1,i} \text{RSS}_i \right|, \left| \sum_{i=1}^{I} \mathbf{f}_{2,i} \text{RSS}_i \right| \cdots, \left| \sum_{i=1}^{I} \mathbf{f}_{L,i} \text{RSS}_i \right| \right\}$$
$$\text{subject to: } lb \leq \text{RSS}_i \leq ub, \tag{19}$$

here, lb and ub represent the lower and upper bounds of the RSS_i measurement range, respectively. Matrix $\mathbf{f}$ has dimensions $L \times I$, where each row contains a pair of 1 and -1, with the condition that no two rows of $\mathbf{f}$ are identical. Additionally, L is restricted to $I - 1$ to account for minimum distances between neighboring RSS values. For example, in an environment with four reference points and $\text{RSS}_1 > \text{RSS}_2 > \text{RSS}_3 > \text{RSS}_4$,

$$\mathbf{f} = \begin{bmatrix} 1 & -1 & 0 & 0 \\ 0 & 1 & -1 & 0 \\ 0 & 0 & 1 & -1 \end{bmatrix}.$$

The optimization (19) can be rewritten as:

$$\max_{C_i} \min \left\{ \left| \mathbf{f}.\ 20\log10\left([C_1, C_2, ..., C_I]^T \right) \right| \right\},$$
$$\text{subject to: } a_i \leq C_i \leq b_i \tag{20}$$

where

$$a_i = \frac{10^{lb/20} - \sum_k B_{k,i}^2 \int_{T1}^{T2} g^2(t - \mu_{k,i})dt}{\alpha_i'^2 \alpha^2},$$

and

$$b_i = \frac{10^{ub/20} - \sum_k B_{k,i}^2 \int_{T1}^{T2} g^2(t - \mu_{k,i})dt}{\alpha_i'^2 \alpha^2}.$$

Apart from the constraints on C_i as mentioned above, additional constraints on equation (19) are necessary to ensure a positive solution. Let $\boldsymbol{\nu}_i$ be a subset of $\boldsymbol{\Upsilon}$ that represents a set of RIS elements chosen for determining the RSS of the ith reference RP. Then,

$$\text{If} \quad \exists \quad j \in I \ \& \ j \neq i, \ \boldsymbol{\nu}_j \subset \boldsymbol{\nu}_i \xrightarrow{\text{then}} C_i > C_j.$$

For any $\boldsymbol{\nu}_j \subset \boldsymbol{\nu}_i$, the condition of $\boldsymbol{\Upsilon} > 0$ results in

$$\mathbf{G}_{i,:}\boldsymbol{\Upsilon} - \mathbf{G}_{j,:}\boldsymbol{\Upsilon} > 0, \tag{21}$$

where $\mathbf{G}_{i,:}$ is the ith row of matrix $\mathbf{G}$. Also, if there exists an h so that $\boldsymbol{\nu}_h \subset \boldsymbol{\nu}_i$ and $\mathbf{G}_{i,:}\boldsymbol{\Upsilon} - \mathbf{G}_{j,:}\boldsymbol{\Upsilon} - \mathbf{G}_{h,:}\boldsymbol{\Upsilon} > 0$, then

$$C_i > C_j + C_h.$$

Suppose that $\boldsymbol{\Psi}$ stands for a set of indexes of $\boldsymbol{\nu}_i$'s subset. For instance, if $\boldsymbol{\nu}_1$ and $\boldsymbol{\nu}_2$ are $\boldsymbol{\nu}_i$'s subsets then, $\boldsymbol{\Psi}$ corresponds to $\{\{1\}, \{2\}, \{1, 2\}\}$ and $\boldsymbol{\nu}_{\boldsymbol{\Psi}_{j,p}} \subset \boldsymbol{\nu}_i$, where $1 \leq p \leq P_j$ and P_j is the length of $\boldsymbol{\Psi}_j$. Then for any $\boldsymbol{\Psi}_j$:

$$if \quad \mathbf{G}_{i,:}\boldsymbol{\Upsilon} - \textstyle\sum_{p=1}^{P_j} \mathbf{G}_{\boldsymbol{\Psi}_{j,p},:}\boldsymbol{\Upsilon} > 0 \quad \Rightarrow \quad C_i > \textstyle\sum_{p=1}^{P_j} C_{\boldsymbol{\Psi}_{j,p}}.$$

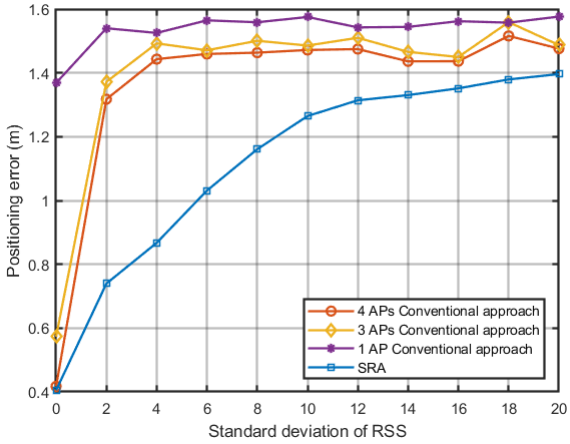

Fig. 4. Comparison of localization error of SRA interacting with 1 AP and the conventional approach in the single and multi-AP scenario.

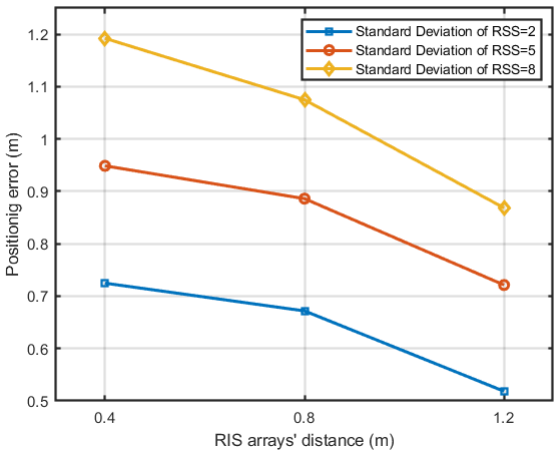

Fig. 5. Comparison of localization error versus different RIS array's separation distance.

The relative coefficients of the constraints on C_i are captured by matrix $\mathbf{A}$. Therefore, the optimization problem can be expressed as follows:

$$\max_{C_i} \left\{ \min \left\{ \left| \mathbf{f}.\ 20\log 10 \left([C_1, C_2, ..., C_I]^T \right) \right| \right\} \right\},$$
$$\text{subject to: } a_i \leq C_i \leq b_i,\ \mathbf{A} \times \mathbf{C} < 0 \qquad (22)$$

where $\mathbf{C} = [C_1, C_2, ..., C_I]^T$. The problem in (22) is solved using Sequential Quadratic Programming (SQL) [10]. Once C_is are determined, $\boldsymbol{\Upsilon}$ is obtained using (15). Having the obtained values of $\mathbf{T}_m$ and $\boldsymbol{\Upsilon}$ the configuration of RIS is accordingly adjusted. Consequently, the MDRSS is customized to the environment with only one RIS configuration. The comparison of 2×2 m indoor environment's radio map with and without RIS manipulating in signal propagation are shown in Fig 3.

V. Simulation Results

In this section, we evaluate the performance of the proposed RIS-aided indoor positioning scheme. The experimental environment consists of a square room measuring $3; \text{m} \times 3; \text{m}$ and divided into 9 RPs, each covering an area of $1; \text{m}^2$. The left corner of the room is considered to be the origin $(0, 0, 0)$ in the xyz plane, and the AP is located at coordinates $(0.1, 0.2, 1)$. The environment is designed to include six multi-path signals reflected from the four side walls, the roof, and the floor, in addition to the Line of Sight (LoS) signal. The RIS, comprising nine elements, is mounted on the plane at a height of $z = 3$ units, which is the height of the room's roof. The center of the RISis located at coordinates $(1.5, 1.5, 3)$.

The RIS is placed on the roof to have an LoS signal from the access point as its main received signal component. A pulse width of $w = 10e^{-9}$ is used, and the measured RSS signal is a combination of LoS, multipath, and signals received from the RIS with Gaussian noise as shown in equation (11). All power gains are assumed to be equal to 1. The positioning accuracy is determined by computing the equation provided below through multiple runs.

$$P_e = \frac{1}{H} \sum_{h \in H} \| p_h^e - p_h^g \|, \qquad (23)$$

where the user's position changes randomly, p_h^e is the estimated position, and p_h^g is the ground truth.

We analyze the positioning accuracy for different parameters corresponding to various system settings. These parameters include the standard deviation of RSS (which is used to evaluate the performance of the system in a noisy environment), the separation distance between the RIS elements, the measurement range of the RSS, and the number of RIS elements.

Fig. 4 illustrates the impact of varying the standard deviation of RSS on the positioning accuracy of a proposed RIS-aided system, which is compared to conventional positioning systems that use different numbers of APs. The RSS measurement range for all systems is between -100 and 0 dB, while the distance between RIS elements is fixed at 0.4 m. The conventional approach employs the Nearest Neighbour (NN) method to match a user's location with the closest pre-measured RSS fingerprints. Our results clearly demonstrate that SRA can effectively cope with high values of RSS standard deviation in noisy scattering environments. Furthermore, our system overperforms conventional multi-AP systems by achieving superior accuracy with just a single AP.

In Fig. 5, we examine the impact of varying the distance between RIS elements on the performance of our proposed system. Specifically, we set the RSS measurement range to $(-100 : 0)$ dB and consider distances of 0.4, 0.8, and 1.2 m between RIS elements. Our results, as shown in Fig. 5, demonstrate that the performance of the system improves with increasing distance between RIS elements. This is because, the farther the RIS elements are, the less probable for RPs to

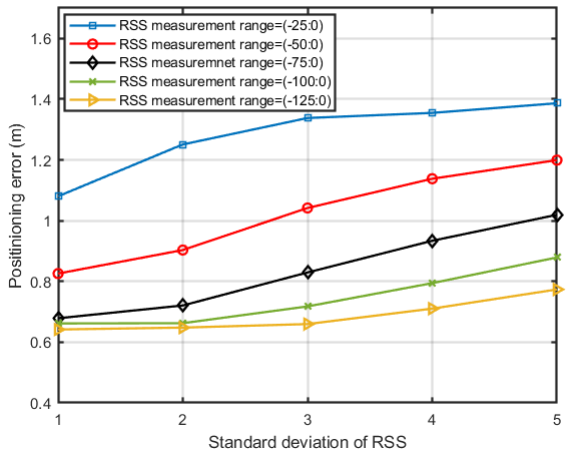

Fig. 6. Effect of different RSS measurement range on SRA localization accuracy where RIS element's distance= 0.8m

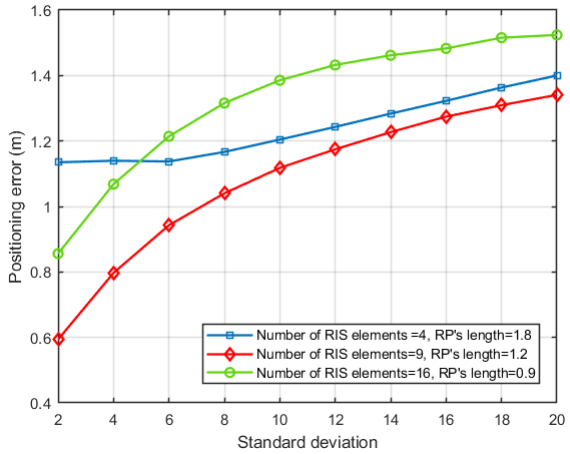

Fig. 7. Comparison of increasing RIS elements. Measurement range $= (-100:0)$ dB, RIS element's distance is the same as RP's length.

have nearly identical values of time delay τ from different RIS elements. As a result, more exclusive vectors $\boldsymbol{\nu}_i$ are assigned to each RP, which reduces interference from neighboring RSS near the borders of RPs and leads to the better overall performance of the system.

Fig. 6 presents the effect of varying the RSS measurement range on the positioning accuracy, with a fixed distance of 0.8 m between RIS elements. Our results show that a wider measurement range leads to higher accuracy in the system. This is because, with a wider range, the maximum differences in RSS values between neighboring RPs are larger, which reduces the likelihood of false positioning. For example, in the measurement range of $(-25:0)$ dB, the maximum difference in RSS values between neighboring RPs is approximately $\left|\frac{-25-0}{9}\right| \simeq 2.8$, whereas it is 11.11 in the range of $(-100:0)$ dB. Therefore, a wider measurement range can effectively handle higher levels of noise in the system.

In Fig. 7, we investigate the effect of varying the number of RIS elements on the performance of our proposed system, in a larger environment of size 3.6×3.6 m^2. We generate different layouts of RPs by creating 2×2, 3×3, and 4×4 layouts, with each RP's length corresponding to 1.8, 1.2, and 0.9, respectively. RSS measurement range is set to $(-100:0)$ dB, and the distance between RIS elements is the same as the length of the RPs.

The simulation's results confirm that increasing the number of RIS elements enhances positioning accuracy by improving the spatial resolution of the environment. Nevertheless, this reduces the maximum differences in RSS values between neighboring RPs. As a result, compared to the 4-element RIS, the 16-element RIS achieves higher (lower) accuracy in low (high) Signal-to-Noise Ratio (SNR) regimes.

VI. Conclusion

We proposed a novel algorithm to enhance localization accuracy by using RIS interacting with an AP. In SRA a combination of RIS elements is selected to customize MDRSS changes from one RP to another without requiring to make a change in the RIS settings. The SRA was implemented by utilizing the Time Differential of Arrival of signals received at an RP from different RIS elements. This was formulated as a max-min optimization problem obtaining the MDRSS. The simulation results confirmed that using the proposed algorithm successfully handles the variance caused by noise, shadowing, and other dynamic properties of the environment, and further outperforms the existing fingerprint-based indoor positioning systems.

References

[1] A. Yassin *et al.*, "Recent advances in indoor localization: A survey on theoretical approaches and applications," *IEEE Communications Surveys Tutorials*, vol. 19, no. 2, pp. 1327–1346, 2017.

[2] T. Tan *et al.*, "An efficient fingerprint database construction approach based on matrix completion for indoor localization," *IEEE Access*, vol. 8, pp. 130 708–130 718, 2020.

[3] K. Kaemarungsi, "Distribution of WLAN received signal strength indication for indoor location determination," in *2006 1st International Symposium on Wireless Pervasive Computing*, 2006, pp. 6 pp.–6.

[4] W. Xue *et al.*, "Improved Wi-Fi RSSI measurement for indoor localization," *IEEE Sensors Journal*, vol. 17, no. 7, pp. 2224–2230, 2017.

[5] E. Basar *et al.*, "Wireless communications through reconfigurable intelligent surfaces," *IEEE Access*, vol. 7, pp. 116 753–116 773, 2019.

[6] C. L. Nguyen *et al.*, "Wireless fingerprinting localization in smart environments using reconfigurable intelligent surfaces," *IEEE Access*, vol. 9, pp. 135 526–135 541, 2021.

[7] T. Ma *et al.*, "Indoor localization with reconfigurable intelligent surface," *IEEE Communications Letters*, vol. 25, no. 1, pp. 161–165, 2021.

[8] H. Zhang *et al.*, "Towards ubiquitous positioning by leveraging reconfigurable intelligent surface," *IEEE Communications Letters*, vol. 25, no. 1, pp. 284–288, 2021.

[9] A. Saleh and R. Valenzuela, "A statistical model for indoor multipath propagation," *IEEE Journal on Selected Areas in Communications*, vol. 5, no. 2, pp. 128–137, 1987.

[10] P. T. Boggs and J. W. Tolle, "Sequential quadratic programming," *Acta numerica*, vol. 4, pp. 1–51, 1995.